A new complex variable meshless method for transient heat conduction problems*

Wang Jian-Fei(王健菲)[a)b)] and Cheng Yu-Min(程玉民)[a)b)†]

[a)] *Shanghai Institute of Applied Mathematics and Mechanics, Shanghai University, Shanghai* 200072, *China*

[b)] *Shanghai Key Laboratory of Mechanics in Energy Engineering, Shanghai University, Shanghai* 200072, *China*

(Received 16 May 2012; revised manuscript received 3 June 2012)

In this paper, based on the improved complex variable moving least-square (ICVMLS) approximation, a new complex variable meshless method (CVMM) for two-dimensional (2D) transient heat conduction problems is presented. The variational method is employed to obtain the discrete equations, and the essential boundary conditions are imposed by the penalty method. As the transient heat conduction problems are related to time, the Crank–Nicolson difference scheme for two-point boundary value problems is selected for the time discretization. Then the corresponding formulae of the CVMM for 2D heat conduction problems are obtained. In order to demonstrate the applicability of the proposed method, numerical examples are given to show the high convergence rate, good accuracy, and high efficiency of the CVMM presented in this paper.

Keywords: meshless method, improved complex variable moving least-square approximation, complex variable meshless method, transient heat conduction problem

PACS: 02.60.Cb, 02.60.Lj, 44.10.+i **DOI:** 10.1088/1674-1056/21/12/120206

1. Introduction

In recent decades, meshless methods have developed so fast that they are now involved in a variety of science and engineering problems.[1−12]

In meshless method, the moving least-square (MLS) approximation[13] is most extensively developed method used to form the shape function. It has been successfully used for simulating a broad range of applications in the last decades.[14−17] The shape function that is formed in the MLS approximation is able to obtain quite a precise solution. However, the MLS approximation is the approximation of a scalar function, leading to the fact that the derived meshless method requires considerable nodes in the domain.

With the view of improving this insufficiency, the improved complex variable moving least-square (ICVMLS) approximation was discussed,[18] and the functional in this method has an explicit physical meaning, which is also an advantage over the complex variable moving least-square (CVMLS) approximation.[19] The ICVMLS approximation is the approximation of a vector function, and thus the trial function of two-dimensional (2D) problems can be formed with a one-dimensional basis function. The number of unknown coefficients in the trial function of the ICVMLS approximation is less than that used in the MLS approximation, and then we can select fewer nodes in the meshless method that is developed from the ICVMLS approximation than in the MLS approximation with no loss of precision.

Heat conduction problems arise in many kinds of engineering applications, and have attracted much attention. Arefmanesh *et al.*[20] and Batra *et al.*[21] put forward a meshless local Petrov–Galerkin method of solving heat conduction problems. Liu *et al.*[22,23] used the meshless least-squares method to solve steady and unsteady state heat conduction problems. Chen and Cheng[24] applied the complex variable reproducing kernel particle method to heat conduction.

In this paper, based on the improved complex variable moving least-square (ICVMLS) approximation, a new complex variable meshless method (CVMM) for 2D transient heat conduction problems is presented. The variational method is employed to obtain the discrete equations, and the essential bound-

*Project supported by the National Natural Science Foundation of China (Grant No. 11171208), the Shanghai Leading Academic Discipline Project, China (Grant No. S30106), and the Innovation Fund for Graduate Student of Shanghai University of China (Grant No. SHUCX120125).

†Corresponding author. E-mail: ymcheng@shu.edu.cn

© 2012 Chinese Physical Society and IOP Publishing Ltd

ary conditions are imposed by the penalty method. As heat conduction problems are related to time, the Crank–Nicolson difference scheme for two-point boundary value problems is selected for the time discretization. Then the corresponding formulae of the CVMM for 2D heat conduction problems are obtained. In order to demonstrate the applicability of the proposed method, numerical examples are given to show the high convergence rate, good accuracy, and high efficiency of the CVMM presented in this paper.

2. Improved complex variable moving least-square approximation

In the ICVMLS approximation, the function $u(z)$ is approximated by $u^h(z)$, which can be expressed as

$$\begin{aligned} u^h(z) &= u_1^h(z) + \mathrm{i}u_2^h(z) \\ &= \sum_{i=1}^{m} \bar{p}_i(z)a_i(z) = \bar{\boldsymbol{p}}^{\mathrm{T}}(z)\boldsymbol{a}(z), \\ z &= x_1 + \mathrm{i}x_2 \in \Omega, \end{aligned} \tag{1}$$

where $\bar{\boldsymbol{p}}^{\mathrm{T}}(z) = (\bar{p}_1(z), \bar{p}_2(z), \ldots, \bar{p}_m(z))$ is the basis function vector which equals the conjugate of the basis function vector $\boldsymbol{p}^{\mathrm{T}}(z) = (p_1(z), p_2(z), \ldots, p_m(z))$, $\boldsymbol{a}^{\mathrm{T}}(z) = (a_1(z), a_2(z), \ldots, a_m(z))$ is the corresponding coefficient vector, and m is the number of terms in the basis function vector.

The local approximation at point z is defined as

$$u^h(z, \hat{z}) = \sum_{i=1}^{m} \bar{p}_i(\hat{z}) \cdot a_i(z) = \bar{\boldsymbol{p}}^{\mathrm{T}}(\hat{z})\boldsymbol{a}(z), \tag{2}$$

where $\hat{z}$ is the node in the local support domain of z and $a_i(z)$ $(i = 1, 2, \ldots, m)$ are determined by minimizing the following functional.

Define a functional as

$$\begin{aligned} J &= \sum_{I=1}^{n} w(z - z_I) \left| u^h(z, z_I) - u(z_I) \right|^2 \\ &= \sum_{I=1}^{n} w(z - z_I) \left(\sum_{i=1}^{m} \bar{p}_i(z_I) \cdot a_i(z) - u(z_I) \right) \\ &\quad \times \overline{\left(\sum_{i=1}^{m} \bar{p}_i(z_I) \cdot a_i(z) - u(z_I) \right)}, \end{aligned} \tag{3}$$

where $w(z - z_I)$ is a weight function with compact support, z_I $(I = 1, 2, \ldots, n)$ are the nodes in a compact support domain of point z and

$$u(z_I) = u_1(z_I) + \mathrm{i}u_2(z_I). \tag{4}$$

For the functions $f(z)$ and $g(z)$, define the inner product as

$$(f, g)_z = \sum_{I=1}^{n} w(z - z_I) f(z_I) \bar{g}(z_I), \quad \forall f, g \in C^0(\bar{\Omega}), \tag{5}$$

where $\bar{g}(z_I)$ is the conjugate of $g(z_I)$, $\bar{\Omega} = \Omega \cup \partial\Omega$, and $C^0(\bar{\Omega})$ is the set of all continuous functions in the domain $\bar{\Omega}$. Correspondingly, the norm is

$$||f||_z = [(f, f)_z]^{1/2}. \tag{6}$$

Equation (3) can be represented as

$$\begin{aligned} J &= (\bar{\boldsymbol{P}}\boldsymbol{a}(z) - \boldsymbol{u}^*(z))^{\mathrm{T}} \boldsymbol{W}(z) \overline{(\bar{\boldsymbol{P}}\boldsymbol{a}(z) - \boldsymbol{u}^*(z))} \\ &= \left\| \bar{\boldsymbol{p}}^{\mathrm{T}}(z) \cdot \boldsymbol{a}(z) - u \right\|_z^2, \end{aligned} \tag{7}$$

where

$$\bar{\boldsymbol{P}} = \begin{bmatrix} \bar{p}_1(z_1) & \bar{p}_2(z_1) & \ldots & \bar{p}_m(z_1) \\ \bar{p}_1(z_2) & \bar{p}_2(z_2) & \ldots & \bar{p}_m(z_2) \\ \vdots & \vdots & \ddots & \vdots \\ \bar{p}_1(z_n) & \bar{p}_2(z_n) & \ldots & \bar{p}_m(z_n) \end{bmatrix}_{n \times m}, \tag{8}$$

$$\boldsymbol{W}(z) = \begin{bmatrix} w(z - z_1) & 0 & \ldots & 0 \\ 0 & w(z - z_2) & \ldots & 0 \\ \vdots & \vdots & \ddots & \vdots \\ 0 & 0 & \ldots & w(z - z_n) \end{bmatrix}, \tag{9}$$

$$\boldsymbol{u}^* = (u(z_1), u(z_2), \ldots, u(z_n))^{\mathrm{T}} = \boldsymbol{Q}\boldsymbol{u}, \tag{10}$$

$$\begin{aligned} \boldsymbol{u} = (&u_1(z_1), u_2(z_1), u_1(z_2), u_2(z_2), \ldots, \\ &u_1(z_n), u_2(z_n))^{\mathrm{T}}, \end{aligned} \tag{11}$$

$$\boldsymbol{Q} = \begin{bmatrix} 1 & \mathrm{i} & 0 & 0 & 0 & 0 & \ldots & 0 & 0 \\ 0 & 0 & 1 & \mathrm{i} & 0 & 0 & \ldots & 0 & 0 \\ 0 & 0 & 0 & 0 & 1 & \mathrm{i} & \ldots & 0 & 0 \\ \vdots & \vdots & \vdots & \vdots & \vdots & \vdots & \ddots & \vdots & \vdots \\ 0 & 0 & 0 & 0 & 0 & 0 & \ldots & 1 & \mathrm{i} \end{bmatrix}_{n \times 2n}. \tag{12}$$

Equation (3) can also be written as

$$J = \left\| a_1\bar{p}_1 + a_2\bar{p}_2 + \cdots + a_m\bar{p}_m - u \right\|_z^2, \tag{13}$$

where $\bar{p}_i = \bar{p}_i(z)$, $i = 1, 2, \ldots, m$.

Let $u^{(1)}$ be the projection of u in the span $(\bar{p}_1, \bar{p}_2, \ldots, \bar{p}_m)$, obviously

$$J^{(1)} = \left\| u^{(1)} - u \right\|_z^2 \tag{14}$$

is the minimum of the functional J.

The function u could be decomposed orthogonally into

$$u = u^{(1)} + u^{(2)}, \tag{15}$$

where $u^{(2)} \perp \text{span}\,(\bar{p}_1, \bar{p}_2, \ldots, \bar{p}_m)$.

Obviously,

$$(\bar{p}_i, u^{(2)})_z = 0, \quad (i = 1, 2, \ldots, m), \tag{16}$$

then we obtain

$$(\bar{p}_i, u)_z = (\bar{p}_i, u^{(1)})_z + (\bar{p}_i, u^{(2)})_z = (\bar{p}_i, u^{(1)})_z, \quad (i = 1, 2, \ldots, m), \tag{17}$$

and

$$\begin{aligned}(\bar{p}_i, u)_z &= (\bar{p}_i, u^{(1)})_z \\ &= (\bar{p}_i, a_1\bar{p}_1 + a_2\bar{p}_2 + \cdots + a_m\bar{p}_m)_z. \end{aligned} \tag{18}$$

The matrix form of Eq. (18) is

$$\begin{bmatrix} (\bar{p}_1, \bar{p}_1)_z & (\bar{p}_1, \bar{p}_2)_z & \ldots & (\bar{p}_1, \bar{p}_m)_z \\ (\bar{p}_2, \bar{p}_1)_z & (\bar{p}_2, \bar{p}_2)_z & \ldots & (\bar{p}_2, \bar{p}_m)_z \\ \vdots & \vdots & \ddots & \vdots \\ (\bar{p}_m, \bar{p}_1)_z & (\bar{p}_m, \bar{p}_2)_z & \ldots & (\bar{p}_m, \bar{p}_m)_z \end{bmatrix} \begin{bmatrix} \bar{a}_1(z) \\ \bar{a}_2(z) \\ \vdots \\ \bar{a}_m(z) \end{bmatrix} = \begin{bmatrix} (\bar{p}_1, u)_z \\ (\bar{p}_2, u)_z \\ \vdots \\ (\bar{p}_m, u)_z \end{bmatrix}, \tag{19}$$

that is

$$(\bar{\boldsymbol{P}}^{\mathrm{T}}\boldsymbol{W}(z)\boldsymbol{P})\bar{\boldsymbol{a}}(z) = \bar{\boldsymbol{P}}^{\mathrm{T}}\boldsymbol{W}(z)\bar{\boldsymbol{u}}^*. \tag{20}$$

The conjugate of Eq. (20) can be written as

$$(\boldsymbol{P}^{\mathrm{T}}\boldsymbol{W}(z)\bar{\boldsymbol{P}})\boldsymbol{a}(z) = \boldsymbol{P}^{\mathrm{T}}\boldsymbol{W}(z)\boldsymbol{u}^*. \tag{21}$$

Solving Eq. (21) for $\boldsymbol{a}(z)$, we obtain

$$\boldsymbol{a}(z) = \boldsymbol{C}^{-1}(z)\boldsymbol{B}(z)\boldsymbol{u}^*, \tag{22}$$

where

$$\boldsymbol{C}(z) = \boldsymbol{P}^{\mathrm{T}}\boldsymbol{W}(z)\bar{\boldsymbol{P}}, \tag{23}$$

$$\boldsymbol{B}(z) = \boldsymbol{P}^{\mathrm{T}}\boldsymbol{W}(z). \tag{24}$$

Combining Eq. (22) with Eq. (2), the final form of the local approximation $u^h(z, \hat{z})$ is written as

$$u^h(z, \hat{z}) = \boldsymbol{\Phi}(z)\boldsymbol{u}^* = \sum_{I=1}^{n} \Phi_I(z)u(z_I), \tag{25}$$

where the shape function $\boldsymbol{\Phi}(z)$ is given by

$$\begin{aligned}\boldsymbol{\Phi}(z) &= (\Phi_1(z), \Phi_2(z), \ldots, \Phi_n(z)) \\ &= \bar{\boldsymbol{p}}^{\mathrm{T}}(z)\boldsymbol{C}^{-1}(z)\boldsymbol{B}(z). \end{aligned} \tag{26}$$

From Eq. (25), we obtain

$$u_1^h(z) = \mathrm{Re}[\boldsymbol{\Phi}(z)\boldsymbol{u}^*] = \mathrm{Re}\left[\sum_{I=1}^{n} \Phi_I(z)u(z_I)\right], \tag{27}$$

$$u_2^h(z) = \mathrm{Im}[\boldsymbol{\Phi}(z)\boldsymbol{u}^*] = \mathrm{Im}\left[\sum_{I=1}^{n} \Phi_I(z)u(z_I)\right]. \tag{28}$$

In the ICVMLS approximation, the trial function of a 2D problem is formed with a one-dimensional basis function; therefore, its number of unknown coefficients is less than the number of the trial functions of the MLS approximation. In the MLS approximation, the linear basis is $\boldsymbol{p}^{\mathrm{T}} = (1, x_1, x_2)$, and three unknown coefficients are included, whereas the ICVMLS approximation is $\bar{\boldsymbol{p}}^{\mathrm{T}} = (1, \bar{z})$, and two unknown coefficients are included. Moreover, in the term of the quadratic basis, the MLS approximation is $\boldsymbol{p}^{\mathrm{T}} = (1, x_1, x_2, x_1^2, x_1x_2, x_2^2)$, and six unknown coefficients are included, whereas the ICVMLS approximation is $\bar{\boldsymbol{p}}^{\mathrm{T}} = (1, \bar{z}, \bar{z}^2)$, and three unknown coefficients are included. In this manner, for an arbitrary point in the domain, we need fewer nodes with domains of influence which cover the point, and thus we can require fewer nodes in the whole domain.

Compared with CVMLS approximation presented by Cheng *et al.*,[19] the ICVMLS approximation has not only all of the excellent features of the former but also a more explicit physical meaning. From the ICVMLS approximation, a distinct expression for the approximating function is obtained. Because of adopting a conjugated polynomial basis to form the shape function, this method has higher computing accuracy and efficiency.[19]

3. CVMM for 2D transient heat conduction problems

The distribution of temperature in the problem is governed by the following equation:

$$\rho c \cdot \frac{\partial T(\boldsymbol{x}, t)}{\partial t} - \frac{\partial}{\partial x_1}\left(k_1 \frac{\partial T(\boldsymbol{x}, t)}{\partial x_1}\right) - \frac{\partial}{\partial x_2}\left(k_2 \frac{\partial T(\boldsymbol{x}, t)}{\partial x_2}\right) - Q = 0, \quad (x \in \Omega), \tag{29}$$

with the boundary conditions

$$T(\boldsymbol{x}, t) - \bar{T} = 0, \quad (x \in \Gamma_1), \tag{30}$$

$$k_1 \frac{\partial T(\boldsymbol{x}, t)}{\partial x_1} n_1 + k_2 \frac{\partial T(\boldsymbol{x}, t)}{\partial x_2} n_2 - \bar{q} = 0, \quad (x \in \Gamma_2), \tag{31}$$

$$k_1 \frac{\partial T(\boldsymbol{x}, t)}{\partial x_1} n_1 + k_2 \frac{\partial T(\boldsymbol{x}, t)}{\partial x_2} n_2 - h(T_a - T(\boldsymbol{x}, t)) = 0,$$

$$(x \in \Gamma_3), \tag{32}$$

and initial condition

$$T(\boldsymbol{x}, 0) = T_0, \tag{33}$$

where $T(\boldsymbol{x}, t)$ is the temperature; t is the time; ρ is the mass density; c is the specific heat; k_1 and k_2 denote the thermal conductivities in the x_1 and x_2 directions, respectively; Q represents the internal heat generation per unit volume; $\bar{T}$ and $\bar{q}$ are the prescribed temperature and density of the heat flux on the corresponding boundary Γ_1 and Γ_2, respectively; h is the convective heat transfer coefficient on the boundary Γ_3; T_a denotes the surrounding fluid temperature under the free convection condition, and the adiabatic boundary temperature under forced convection condition; Ω is the 2D domain bounded by Γ, with $\Gamma = \Gamma_1 \cup \Gamma_2 \cup \Gamma_3$; n_1 and n_2 are the unit normal vectors pointing outward to the boundary in the x_1 and x_2 directions, respectively.

The transient heat conduction problem can be regarded as a definite solution of a parabolic equation. In a transient state, T and $\partial T/\partial t$ are functions determined only by coordinates, then transient heat conduction problem can be regarded as a steady-state heat conduction problem, which can be seen as the boundary value problem of an elliptic equation.

The equivalent functional is

$$\begin{aligned}\Pi =& \int_\Omega \left[T\left(\rho c \frac{\partial T}{\partial t} - Q\right)\right] \mathrm{d}\Omega \\ &+ \int_\Omega \left[\frac{1}{2}k_1\left(\frac{\partial T}{\partial x_1}\right)^2 + \frac{1}{2}k_2\left(\frac{\partial T}{\partial x_2}\right)^2\right] \mathrm{d}\Omega \\ &+ \int_{\Gamma_2} T\bar{q}\,\mathrm{d}\Gamma + \int_{\Gamma_3} h\left(\frac{T^2}{2} - TT_a\right) \mathrm{d}\Gamma. \end{aligned} \tag{34}$$

The field function T, which makes $\delta\Pi$ reach zero, is exactly the solution satisfying control equation (29), and boundary conditions (31) and (32). Imposing essential boundary condition (30) by the penalty method, we obtain the modified functional as

$$\Pi^* = \Pi + \frac{1}{2}\int_{\Gamma_1} (T - \bar{T})\alpha(T - \bar{T})\,\mathrm{d}\Gamma, \tag{35}$$

where α is the penalty factor.

Taking the variation of Eq. (35), we have

$$\delta\Pi^* = \delta\Pi + \int_{\Gamma_1} \delta(T - \bar{T})\alpha(T - \bar{T})\,\mathrm{d}\Gamma. \tag{36}$$

Substituting Eq. (34) into Eq. (36) yields

$$\begin{aligned}\delta\Pi^* =& \int_\Omega \delta T \cdot \rho c \cdot \frac{\partial T}{\partial t}\,\mathrm{d}\Omega \\ &+ \int_\Omega \delta(\boldsymbol{L}T)^{\mathrm{T}} \cdot \tilde{\boldsymbol{k}} \cdot (\boldsymbol{L}T)\,\mathrm{d}\Omega \\ &- \int_\Omega \delta T \cdot Q\,\mathrm{d}\Omega - \int_{\Gamma_2} \delta T \cdot \bar{q}\,\mathrm{d}\Gamma \\ &- \int_{\Gamma_3} \delta T \cdot h \cdot (T_a - T)\,\mathrm{d}\Gamma \\ &+ \int_{\Gamma_1} \delta T \cdot \alpha \cdot T\,\mathrm{d}\Gamma - \int_{\Gamma_1} \delta T \cdot \alpha \cdot \bar{T}\,\mathrm{d}\Gamma, \end{aligned} \tag{37}$$

where

$$\tilde{\boldsymbol{k}} = \begin{bmatrix} k_1 & 0 \\ 0 & k_2 \end{bmatrix}, \tag{38}$$

$$\boldsymbol{L}(\cdot) = \begin{bmatrix} \dfrac{\partial}{\partial x_1} \\ \dfrac{\partial}{\partial x_2} \end{bmatrix} (\cdot). \tag{39}$$

The essential difference between steady- and unsteady-state heat conduction problems is that the temperature is not only a function of space coordinates, but also related to time. Because the time and space domain are not coupled, we apply the CVMM to the space, and the finite difference method to the time. Starting from the initial temperature, we solve the temperature of the next moment after one time step, and then the temperature at any time can be achieved step by step.

From Eq. (27), we can obtain the approximation of the temperature function as

$$\begin{aligned} T(z,t) &= \mathrm{Re}[\boldsymbol{\Phi}(z)\boldsymbol{T}(t)] = \sum_{I=1}^{n} \mathrm{Re}[\Phi_I(z)] \cdot T_I(t) \\ &= \sum_{I=1}^{n} \tilde{\Phi}_I(z) \cdot T_I(t) = \tilde{\boldsymbol{\Phi}}(z)\boldsymbol{T}, \end{aligned} \tag{40}$$

$$\begin{aligned} \frac{\partial T(z,t)}{\partial t} &= \frac{\partial}{\partial t}\sum_{I=1}^{n} \tilde{\Phi}_I(z) \cdot T_I(t) \\ &= \sum_{I=1}^{n} \tilde{\Phi}_I(z) \cdot \frac{\partial T_I(t)}{\partial t} = \tilde{\boldsymbol{\Phi}}(z)\dot{\boldsymbol{T}}, \end{aligned} \tag{41}$$

where n is the node number in the compact support domain of z, and

$$\tilde{\boldsymbol{\Phi}}(z) = (\tilde{\Phi}_1(z), \tilde{\Phi}_2(z), \ldots, \tilde{\Phi}_n(z)), \tag{42}$$

$$\tilde{\Phi}_I(z) = \mathrm{Re}[\Phi_I(z)], \tag{43}$$

$$\boldsymbol{T} = (T_1(t), T_2(t), \ldots, T_n(t))^{\mathrm{T}}, \tag{44}$$

$$\dot{\boldsymbol{T}} = \left(\frac{\partial T_1(t)}{\partial t}, \frac{\partial T_2(t)}{\partial t}, \ldots, \frac{\partial T_n(t)}{\partial t}\right)^{\mathrm{T}}, \tag{45}$$

$$\boldsymbol{L}T(z,t) = \sum_{I=1}^{n} \begin{bmatrix} \dfrac{\partial}{\partial x_1} \\ \dfrac{\partial}{\partial x_2} \end{bmatrix} \mathrm{Re}[\Phi_I(z)] \cdot T_I(t)$$

$$= \sum_{I=1}^{n} \boldsymbol{B}_I(z) \cdot T_I(t) = \boldsymbol{B}(z) \cdot \boldsymbol{T}. \quad (46)$$

Substituting Eqs. (40), (41), and (46) into Eq. (37) yields

$$\begin{aligned}\delta \Pi^* = & \int_{\Omega} \delta[\tilde{\boldsymbol{\Phi}}(z)\boldsymbol{T}] \cdot \rho c \cdot [\tilde{\boldsymbol{\Phi}}(z)\dot{\boldsymbol{T}}] \mathrm{d}\Omega \\ & + \int_{\Omega} \delta[\boldsymbol{B}(z)\boldsymbol{T}]^{\mathrm{T}} \cdot \tilde{\boldsymbol{k}} \cdot [\boldsymbol{B}(z)\boldsymbol{T}] \mathrm{d}\Omega \\ & - \int_{\Omega} \delta[\tilde{\boldsymbol{\Phi}}(z)\boldsymbol{T}] \cdot Q \mathrm{d}\Omega \\ & - \int_{\Gamma_2} \delta[\tilde{\boldsymbol{\Phi}}(z)\boldsymbol{T}] \cdot \bar{q} \mathrm{d}\Gamma \\ & - \int_{\Gamma_3} \delta[\tilde{\boldsymbol{\Phi}}(z)\boldsymbol{T}] \cdot h \cdot T_a \mathrm{d}\Gamma \\ & + \int_{\Gamma_3} \delta[\tilde{\boldsymbol{\Phi}}(z)\boldsymbol{T}] \cdot h \cdot [\tilde{\boldsymbol{\Phi}}(z)\boldsymbol{T}]) \mathrm{d}\Gamma \\ & + \int_{\Gamma_1} \delta[\tilde{\boldsymbol{\Phi}}(z)\boldsymbol{T}] \cdot \alpha \cdot [\tilde{\boldsymbol{\Phi}}(z)\boldsymbol{T}] \mathrm{d}\Gamma \\ & - \int_{\Gamma_1} \delta[\tilde{\boldsymbol{\Phi}}(z)\boldsymbol{T}] \cdot \alpha \cdot \bar{T} \mathrm{d}\Gamma. \end{aligned} \quad (47)$$

To obtain discrete system equations, the integral terms in Eq. (47) will be analyzed as follows.

The first integral term of Eq. (47) is

$$\begin{aligned} & \int_{\Omega} \delta[\tilde{\boldsymbol{\Phi}}(z)\boldsymbol{T}] \cdot \rho c \cdot [\tilde{\boldsymbol{\Phi}}(z)\dot{\boldsymbol{T}}] \mathrm{d}\Omega \\ = & \delta \boldsymbol{T}^{\mathrm{T}} \cdot \left[\int_{\Omega} \tilde{\boldsymbol{\Phi}}^{\mathrm{T}}(z) \rho c \tilde{\boldsymbol{\Phi}}(z) \mathrm{d}\Omega \right] \dot{\boldsymbol{T}} = \delta \boldsymbol{T}^{\mathrm{T}} \cdot C \dot{\boldsymbol{T}}, \end{aligned} \quad (48)$$

where heat capacity matrix $\boldsymbol{C}$ is

$$\boldsymbol{C} = \int_{\Omega} \tilde{\boldsymbol{\Phi}}^{\mathrm{T}}(z) \rho c \tilde{\boldsymbol{\Phi}}(z) \mathrm{d}\Omega. \quad (49)$$

The second integral term of Eq. (47) is

$$\begin{aligned} & \int_{\Omega} \delta[\boldsymbol{B}(z)\boldsymbol{T}]^{\mathrm{T}} \cdot \tilde{\boldsymbol{k}} \cdot [\boldsymbol{B}(z)\boldsymbol{T}] \mathrm{d}\Omega \\ = & \delta \boldsymbol{T}^{\mathrm{T}} \cdot \left[\int_{\Omega} \boldsymbol{B}^{\mathrm{T}}(z) \tilde{\boldsymbol{k}} \boldsymbol{B}(z) \mathrm{d}\Omega \right] \boldsymbol{T} = \delta \boldsymbol{T}^{\mathrm{T}} \cdot \boldsymbol{K} \boldsymbol{T}, \end{aligned} \quad (50)$$

where thermal conductivity matrix $\boldsymbol{K}$ is

$$\boldsymbol{K} = \int_{\Omega} \boldsymbol{B}^{\mathrm{T}}(z) \tilde{\boldsymbol{k}} \boldsymbol{B}(z) \mathrm{d}\Omega. \quad (51)$$

The third integral term of Eq. (47) is

$$\begin{aligned} & \int_{\Omega} \delta[\tilde{\boldsymbol{\Phi}}(z)\boldsymbol{T}] \cdot Q \mathrm{d}\Omega \\ = & \delta \boldsymbol{T}^{\mathrm{T}} \cdot \int_{\Omega} \tilde{\boldsymbol{\Phi}}^{\mathrm{T}}(z) Q \mathrm{d}\Omega = \delta \boldsymbol{T}^{\mathrm{T}} \cdot \boldsymbol{F}^{(1)}, \end{aligned} \quad (52)$$

where $\boldsymbol{F}^{(1)}$ is a thermal load vector caused by heat source, and

$$\boldsymbol{F}^{(1)} = \int_{\Omega} \tilde{\boldsymbol{\Phi}}^{\mathrm{T}}(z) Q \mathrm{d}\Omega. \quad (53)$$

The fourth integral term of Eq. (47) is

$$\begin{aligned} & \int_{\Gamma_2} \delta[\tilde{\boldsymbol{\Phi}}(z)\boldsymbol{T}] \cdot \bar{q} \mathrm{d}\Gamma \\ = & \delta \boldsymbol{T}^{\mathrm{T}} \cdot \int_{\Gamma_2} \tilde{\boldsymbol{\Phi}}^{\mathrm{T}} \bar{q} \mathrm{d}\Gamma = \delta \boldsymbol{T}^{\mathrm{T}} \cdot \boldsymbol{F}^{(2)}, \end{aligned} \quad (54)$$

where $\boldsymbol{F}^{(2)}$ is a thermal load vector caused by constant heat flux, and

$$\boldsymbol{F}^{(2)} = \int_{\Gamma_2} \tilde{\boldsymbol{\Phi}}^{\mathrm{T}} \bar{q} \mathrm{d}\Gamma. \quad (55)$$

The fifth integral term of Eq. (47) is

$$\begin{aligned} & \int_{\Gamma_3} \delta[\tilde{\boldsymbol{\Phi}}(z)\boldsymbol{T}] \cdot h \cdot T_a \mathrm{d}\Gamma \\ = & \delta \boldsymbol{T}^{\mathrm{T}} \cdot \int_{\Gamma_3} \tilde{\boldsymbol{\Phi}}^{\mathrm{T}}(z) h T_a \mathrm{d}\Gamma = \delta \boldsymbol{T}^{\mathrm{T}} \cdot \boldsymbol{F}^{(3)}, \end{aligned} \quad (56)$$

where $\boldsymbol{F}^{(3)}$ is a thermal load vector caused by heat exchange, and

$$\boldsymbol{F}^{(3)} = \int_{\Gamma_3} \tilde{\boldsymbol{\Phi}}^{\mathrm{T}}(z) h T_a \mathrm{d}\Gamma. \quad (57)$$

The sixth integral term of Eq. (47) is

$$\begin{aligned} & \int_{\Gamma_3} \delta[\tilde{\boldsymbol{\Phi}}(z)\boldsymbol{T}] \cdot h \cdot [\tilde{\boldsymbol{\Phi}}(z)\boldsymbol{T}] \mathrm{d}\Gamma \\ = & \delta \boldsymbol{T}^{\mathrm{T}} \cdot \left[\int_{\Gamma_3} \tilde{\boldsymbol{\Phi}}^{\mathrm{T}}(z) h \tilde{\boldsymbol{\Phi}}(z) \mathrm{d}\Gamma \right] \boldsymbol{T} = \delta \boldsymbol{T}^{\mathrm{T}} \cdot \boldsymbol{H} \boldsymbol{T}, \end{aligned} \quad (58)$$

where

$$\boldsymbol{H} = \int_{\Gamma_3} \tilde{\boldsymbol{\Phi}}^{\mathrm{T}}(z) h \tilde{\boldsymbol{\Phi}}(z) \mathrm{d}\Gamma. \quad (59)$$

The seventh integral term of Eq. (47) is

$$\begin{aligned} & \int_{\Gamma_1} \delta[\tilde{\boldsymbol{\Phi}}(z)\boldsymbol{T}] \cdot \alpha \cdot [\tilde{\boldsymbol{\Phi}}(z)\boldsymbol{T}] \mathrm{d}\Gamma \\ = & \delta \boldsymbol{T}^{\mathrm{T}} \cdot \left[\int_{\Gamma_1} \tilde{\boldsymbol{\Phi}}^{\mathrm{T}}(z) \alpha \tilde{\boldsymbol{\Phi}}(z) \mathrm{d}\Gamma \right] \boldsymbol{T} \\ = & \delta \boldsymbol{T}^{\mathrm{T}} \cdot \boldsymbol{K}^{\alpha} \boldsymbol{T}, \end{aligned} \quad (60)$$

where

$$\boldsymbol{K}^{\alpha} = \int_{\Gamma_1} \tilde{\boldsymbol{\Phi}}^{\mathrm{T}}(z) \alpha \tilde{\boldsymbol{\Phi}}(z) \mathrm{d}\Gamma. \quad (61)$$

The eighth integral term of Eq. (47) is

$$\begin{aligned} & \int_{\Gamma_1} \delta[\tilde{\boldsymbol{\Phi}}(z)\boldsymbol{T}] \cdot \alpha \cdot \bar{T} \mathrm{d}\Gamma \\ = & \delta \boldsymbol{T}^{\mathrm{T}} \cdot \int_{\Gamma_1} \tilde{\boldsymbol{\Phi}}^{\mathrm{T}}(z) \alpha \bar{T} \mathrm{d}\Gamma = \delta \boldsymbol{T}^{\mathrm{T}} \cdot \boldsymbol{F}^{\alpha}, \end{aligned} \quad (62)$$

where

$$\boldsymbol{F}^{\alpha} = \int_{\Gamma_1} \tilde{\boldsymbol{\Phi}}^{\mathrm{T}}(z)\alpha\bar{T}\,\mathrm{d}\Gamma. \tag{63}$$

Substituting Eqs. (48), (50), (52), (54), (56), (58), (60), and (62) into Eq. (47) yields

$$\begin{aligned}\delta\Pi^* = {} & \delta\boldsymbol{T}^{\mathrm{T}} \cdot (\boldsymbol{C}\dot{\boldsymbol{T}} + \boldsymbol{K}\boldsymbol{T} + \boldsymbol{H}\boldsymbol{T} + \boldsymbol{K}^{\alpha}\boldsymbol{T} \\ & - \boldsymbol{F}^{(1)} - \boldsymbol{F}^{(2)} - \boldsymbol{F}^{(3)} - \boldsymbol{F}^{\alpha}).\end{aligned} \tag{64}$$

As $\delta\Pi^* = 0$ and due to the arbitrariness of $\delta\boldsymbol{T}^{\mathrm{T}}$ in Eq. (64), we can obtain the final linear system as

$$\boldsymbol{C}\dot{\boldsymbol{T}} + \bar{\boldsymbol{K}}\boldsymbol{T} = \bar{\boldsymbol{F}}, \tag{65}$$

$$\bar{\boldsymbol{K}} = \boldsymbol{K} + \boldsymbol{H} + \boldsymbol{K}^{\alpha}, \tag{66}$$

$$\bar{\boldsymbol{F}} = \boldsymbol{F}^{(1)} + \boldsymbol{F}^{(2)} + \boldsymbol{F}^{(3)} + \boldsymbol{F}^{\alpha}. \tag{67}$$

Equation (65) is a linear system of ordinary differential equations, in which time is the only independent variable. Suppose that the time step is Δt, using the traditional difference method for two-point boundary value problems, we can establish the relation of $T_{t+\Delta t}$ and T_t as

$$\theta\left(\frac{\partial T}{\partial t}\right)_{t+\Delta t} + (1-\theta)\left(\frac{\partial T}{\partial t}\right)_{t} = \frac{T_{t+\Delta t} - T_t}{\Delta t}. \tag{68}$$

Solving Eq. (65) for $(\partial T/\partial t)_{t+\Delta t}$ and $(\partial T/\partial t)_t$, respectively, and substituting the results into Eq. (68), as C is independent of time, we obtain

$$\begin{aligned}&\left(\frac{\boldsymbol{C}}{\Delta t} + \theta\bar{\boldsymbol{K}}_{t+\Delta t}\right)\boldsymbol{T}_{t+\Delta t} \\ &= \left(\frac{\boldsymbol{C}}{\Delta t} - (1-\theta)\bar{\boldsymbol{K}}_t\right)\boldsymbol{T}_t + \theta\bar{\boldsymbol{F}}_{t+\Delta t} + (1-\theta)\bar{\boldsymbol{F}}_t,\end{aligned} \tag{69}$$

where θ is a time weighed coefficient, of which the different values correspond to different time difference forms. When $\theta = 0$, it is the forward difference scheme, i.e.,

$$\left(\boldsymbol{C}\frac{\boldsymbol{T}_{t+\Delta t} - \boldsymbol{T}_t}{\Delta t}\right) + \bar{\boldsymbol{K}}_t\boldsymbol{T}_t = \bar{\boldsymbol{F}}_t; \tag{70}$$

when $\theta = 1/2$, it is the C–N (Crank–Nicolson) scheme,

$$\begin{aligned}&\left(\boldsymbol{C}\frac{\boldsymbol{T}_{t+\Delta t} - \boldsymbol{T}_t}{\Delta t}\right) + \frac{1}{2}\left(\bar{\boldsymbol{K}}_{t+\Delta t}\boldsymbol{T}_{t+\Delta t} + \bar{\boldsymbol{K}}_t\boldsymbol{T}_t\right) \\ &= \frac{1}{2}\left(\bar{\boldsymbol{F}}_{t+\Delta t} + \bar{\boldsymbol{F}}_t\right);\end{aligned} \tag{71}$$

and when $\theta = 1$, the backward difference scheme is obtained as

$$\left(\boldsymbol{C}\frac{\boldsymbol{T}_{t+\Delta t} - \boldsymbol{T}_t}{\Delta t}\right) + \bar{\boldsymbol{K}}_{t+\Delta t}\boldsymbol{T}_{t+\Delta t} = \bar{\boldsymbol{F}}_{t+\Delta t}. \tag{72}$$

Supposing that time step is $\Delta t = 0.05$ s, the cases $\theta = 1/2$, $\theta = 0$, and $\theta = 1$ are all computed as simple examples. The numerical result of $\theta = 1/2$ coincides especially well with the analytical solution, and in fact cannot be distinguished from the analytical solution. Then we draw a conclusion that the result of the C–N scheme is more accurate than those of the other difference schemes in the heat conduction problems.

4. Numerical examples

In this section, we investigate the use of the CVMM to solve 2D heat conduction examples. The node distribution for each example is regular, and the linear basis function and a 4×4 Gauss quadrature are employed. The cubic spline weight function used in the present analysis can be written as follows:

$$w(d) = \begin{cases} \dfrac{2}{3} - 4d^2 + 4d^3, & \text{for } d \le \dfrac{1}{2}, \\ \dfrac{4}{3} - 4d + 4d^2 - \dfrac{4}{3}d^3, & \text{for } \dfrac{1}{2} < d \le 1, \\ 0, & \text{for } d > 1, \end{cases} \tag{73}$$

where $d = d_I/d_{mI}$, with $d_I = \|z - z_I\|$, d_{mI} being the radius of support domain of z_I.

For the purpose of error estimation and convergence studies, the relative error is defined as

$$r = \sum_i \left|\frac{u_i^{\mathrm{num}} - u_i^{\mathrm{exact}}}{u_i^{\mathrm{exact}}}\right|^2. \tag{74}$$

4.1. 2D heat conduction with Dirichlet boundary conditions

Consider a problem in a square, the control equation is

$$\begin{aligned}&\frac{\partial T(x_1,x_2,t)}{\partial t} - \frac{\partial^2 T(x_1,x_2,t)}{\partial x_1^2} - \frac{\partial^2 T(x_1,x_2,t)}{\partial x_2^2} = 0, \\ &x_1 \in [0,1], x_2 \in [0,1],\end{aligned} \tag{75}$$

with the boundary conditions

$$T(0,x_2,t) = \mathrm{e}^{-2t}\sin x_2,$$

$$T(1,x_2,t) = \mathrm{e}^{-2t}\sin(1+x_2), \tag{76}$$

$$T(x_1,0,t) = \mathrm{e}^{-2t}\sin x_1,$$

$$T(x_1,1,t) = \mathrm{e}^{-2t}\sin(1+x_1), \tag{77}$$

and the initial condition

$$T(x_1,x_2,0) = \sin(x_1+x_2). \tag{78}$$

The analytical solution of this problem is

$$T(x_1, x_2, t) = \mathrm{e}^{-2t}\sin(x_1 + x_2). \tag{79}$$

As shown in Fig. 1, 11×11 nodes are uniformly distributed in the domain $\Omega = [0, 1] \times [0, 1]$. The following parameters are employed in solving this problem, that is, penalty factor is $\alpha = 1.0 \times 10^3$, scaling parameter is $d_{\max} = 1.5$, and the time step is $\Delta t = 0.001$ s.

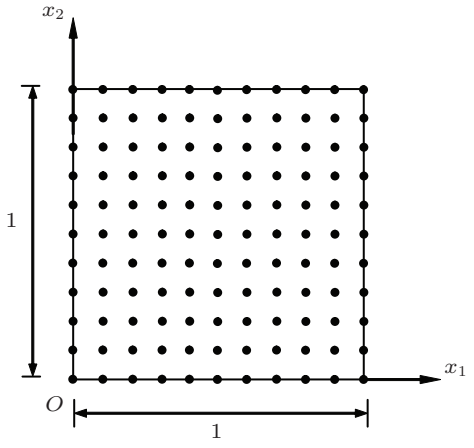


Fig. 1. Node distribution.

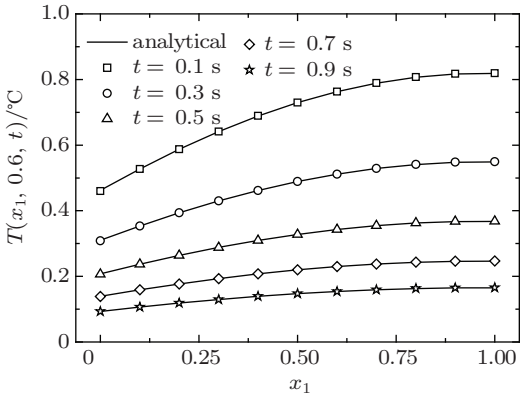


Fig. 2. Heat distributions with time at $x_2 = 0.6$.

Figures 2 and 3 show the solutions of the heat distribution at x_1 and x_2 directions, respectively, at different times. In addition, the relationship between numbers of nodes and relative error at $x_1 = 0.5$ and $t = 0.2$ s is given in Fig. 4, which shows that the solution converges as the number of nodes increases, and 13×13 nodes gives excellent results. The present results show that the CVMM not only obtains excellent solutions under different times, but also has good convergence characteristics.

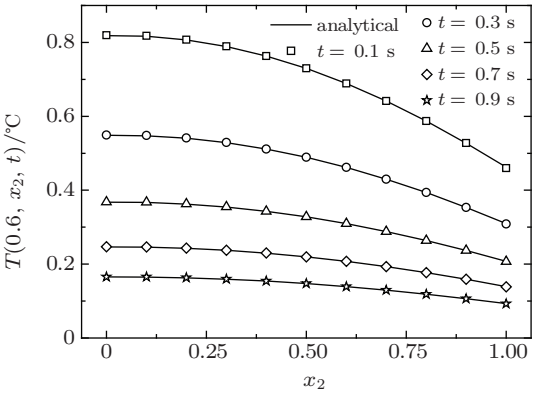


Fig. 3. Heat distributions with time at $x_1 = 0.6$.

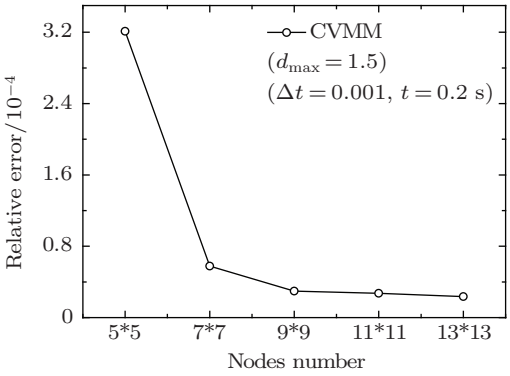


Fig. 4. Convergence rates of the CVMM with different numbers of nodes.

Comparisons between the analytical solutions and the numerical solutions by the CVMM and the EFG method at $x_1 = 0.5$ and $x_2 = 0.5$ are presented in Figs. 5 and 6, respectively. Table 1 shows the relative errors and CPU times with the EFG method and the CVMM, for the example calculated at $x_1 = 0.5$.

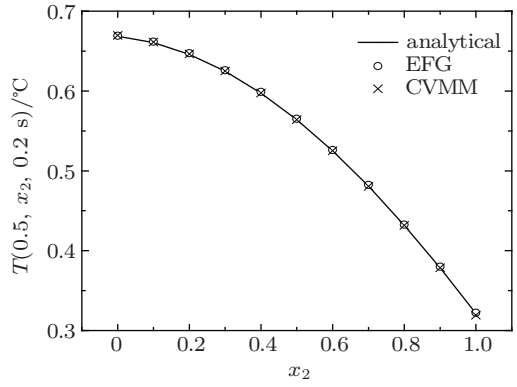


Fig. 5. Heat distribution at $x_1 = 0.5$ and $t = 0.2$ s.

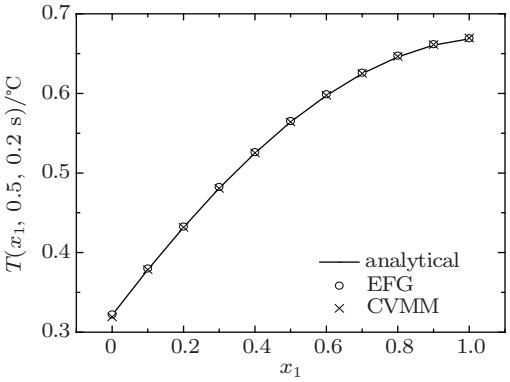


Fig. 6. Heat distribution at $x_2 = 0.5$ and $t = 0.2$ s.

Table 1. Comparison between EFG method and CVMM.

t/s	CVMM		EFG	
	$r/10^{-5}$	CPU time/s	$r/10^{-5}$	CPU time/s
0.1	4.8345	13.968439	6.5078	27.024245
0.3	4.8655	35.285811	6.5345	71. 284678
0.5	4.8664	52.798336	6.5908	116.273410
0.7	4.8665	72.732437	6.5925	162.221989
0.9	4.8655	104.589538	6.5925	216.177227

From the above plots and table, it is shown that the CPU time of the EFG method is nearly twice as much as that of the CVMM, and the relative errors of the EFG method are totally over 25% of the CVMM's.

4.2. 2D heat conduction with Robin boundary condition

Consider a cube with a length of 20 m and a width of 10 m, and its thickness is a unit value. The initial temperature is T_0 =20 °C throughout the cube, and all the other boundaries are maintained at the temperature T_a = 100 °C. The top and bottom surface are insulated, and the left and right surfaces are both subjected to an inflow heat flux of magnitude h = 1600 W/(m^2 · °C). The thermal conductivity is $k_1 = k_2$ = 16 W/(m·°C), specific heat capacity is $\rho c = 10^6$ J/(m^3 · °C), and no source exists in the domain.

On account of unit thickness of the cube, this example is a 2D problem in essence. As presented in Fig. 7, a 21×13 uniform node distribution is arranged in the rectangular domain Ω. In the computation, a support size is selected as 1.7 times the minimum distance of nodes.

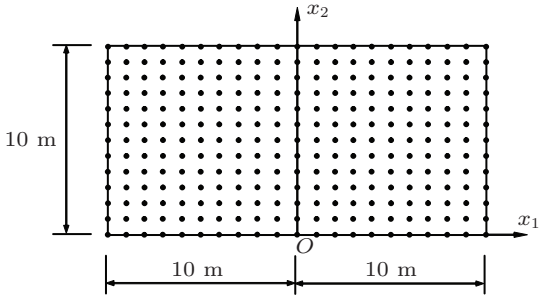


Fig. 7. Node distribution.

Considering the symmetry of the problem, we select three typical nodes, which are $A(0, 0)$, $B(5, 5)$, and $C(10, 0)$, to calculate at t = 1 s, 2 s, and 3 s separately. Table 2 lists the numerical results of the CVMM, the EFG method, and the CVEFG method. From the relative errors of the three methods, we find that although these methods are all quantitatively in agreement with the exact solution, the result of the CVMM is much more accurate than the other ones, and the relative error of the CVMM is even less than one tenth of the other methods at some points.

Therefore, a conclusion can be drawn that the CVMM has good convergence rate and better accuracy and efficiency than the EFG and CVEFG methods.

Table 2. Comparison among results obtained with three methods.

t/s	Point	Exact	CVMM		CVEFG		EFG	
			Numerical/°C	$r/10^{-5}$	Numerical/°C	$r/10^{-5}$	Numerical/°C	$r/10^{-5}$
1.0	A	22.304	22.288	0.0514	22.241	0.7978	22.252	0.5436
	B	27.456	27.439	0.0383	27.491	0.1650	27.410	0.2807
	C	46.384	46.423	0.0707	46.555	1.3591	46.189	1.7674
2.0	A	29.344	29.447	1.2321	29.517	3.4758	29.564	5.6209
	B	35.776	35.754	0.0378	35.858	0.5253	35.703	0.4164
	C	53.928	53.833	0.3103	53.833	0.3103	53.632	3.0127
3.0	A	37.232	37.330	0.6928	37.439	3.0911	37.424	2.6593
	B	42.944	42.980	0.0703	43.299	6.8336	42.891	0.1523
	C	59.072	59.212	0.5617	59.257	0.9808	59.222	0.6448

5. Conclusions

The ICVMLS approximation we proposed has an explicit physical meaning and greater computational accuracy and efficiency. Combining the ICVMLS approximation with the variational method, the CVMM for 2D transient heat conduction problems is presented. Two numerical examples are given to show the validity of the CVMM and its relevant results. And the CVMM has the advantages of good convergence rate, and higher computational accuracy and efficiency over the EFG and CVEFG method.

References

[1] Belytschko T, Krongauz Y, Organ D, Fleming M and Krysl P 1996 *Comput. Methods Appl. Mech. Engrg.* **139** 3

[2] Qin Y X and Cheng Y M 2006 *Acta Phys. Sin.* **55** 3215 (in Chinese)

[3] Cheng R J and Cheng Y M 2011 *Acta Phys. Sin.* **60** 070206 (in Chinese)

[4] Li S C, Cheng Y M and Li S C 2006 *Acta Phys. Sin.* **55** 4760 (in Chinese)

[5] Cheng Y and Li J 2006 *Sci. Chin.* G: *Phys. Mech. & Astron.* **49** 46

[6] Li D M, Peng M J and Cheng Y M 2011 *Sci. Chin.: Phys. Mech. & Astron.* **41** 1003 (in Chinese)

[7] Dai B D and Cheng Y M 2007 *Acta Phys. Sin.* **56** 597 (in Chinese)

[8] Cheng R J and Cheng Y M 2008 *Acta Phys. Sin.* **57** 6037 (in Chinese)

[9] Cheng R J and Cheng Y M 2011 *Chin. Phys.* B **20** 070206

[10] Chen L and Cheng Y M 2010 *Chin. Phys.* B **19** 090204

[11] Cheng Y M and Li J H 2005 *Acta Phys. Sin.* **54** 4463 (in Chinese)

[12] Chen L and Cheng Y M 2008 *Acta Phys. Sin.* **57** 1 (in Chinese)

[13] Lancaster P and Salkauskas K 1981 *Math. Comput.* **37** 141

[14] Afshar M H, Naisipour M and Amani J 2011 *Finite Elem. Anal. Des.* **47** 1315

[15] Wang J F, Bai F N and Cheng Y M 2011 *Chin. Phys.* B **20** 030206

[16] Zhang Z, Zhao P and Liew K M 2009 *Eng. Anal. Bound. Elem.* **33** 547

[17] Ren H P, Cheng Y M and Zhang W 2009 *Chin. Phys.* B **18** 4065

[18] Bai F N, Li D M, Wang J F and Cheng Y M 2012 *Chin. Phys.* B **21** 020204

[19] Cheng Y M, Peng M J and Li J H 2005 *Chin. J. Theor. Appl. Mech.* **37** 719 (in Chinese)

[20] Arefmanesh A, Najafi M and Abdi H 2005 *J. Fluid Eng.* **127** 647

[21] Batra R C, Porfiri M and Spinello D 2004 *Int. J. Numer. Method Eng.* **61** 2461

[22] Liu Y, Zhang X and Lu M W 2005 *Tsinghua Sci. Tech.* **10** 61

[23] Liu Y, Zhang X and Lu M W 2005 *Numer. Heat Transfer* B: *Fund.* **47** 257

[24] Chen L and Cheng Y M 2008 *Acta Phys. Sin.* **57** 6047 (in Chinese)